Numerical simulation of orbital debris impact on spacecraft

G. Pezzica[a], R.Destefanis[b], M. Faraud[b]
[a]*Sigma Epsilon S.r.l, Via Chiusura 16, 54028 Villafranca Lunigiana (MS), Italy*
[b]*Alenia Spazio S.p.A., Corso Marche 41, 10146 Torino, Italy*

Abstract

The non-linear explicit finite-differences computer code AUTODYN-2D[1] has been used for modelling the hypervelocity impact of an aluminium projectile against a 3-wall structure made of aluminium alloy (two bumper shields and a rear or back-up wall, with stand-off distances in between). The target configuration has been chosen to assess the resistance to debris impact of a protection system under investigation for a manned module to be attached to the International Space Station Alpha. The hydrocode calculations have been compared with the hypervelocity impact experiment of a spherical projectile, 1.0 cm in diameter, hitting the target at 7 km/s. The perforation of the first bumper shield, the phase transition of the projectile material, the interaction of the debris cloud with the second bumper shield and the impact of the spalling fragments against the back-up wall have been investigated.

1 Introduction

Damages to spacecraft, and especially manned modules, due to orbital debris nowadays arouse great interest. A conventional protection against this threat is obtained by using aluminium "Whipple shields", consisting of two plates separated by a space (stand-off). Protection being equal, a Whipple shield allows a considerable weight reduction with respect to a single plate, in which the whole impacting momentum is localised in a small area. On the contrary, in the Whipple shield the first sheet (the first bumper shield) breaks up the projectile into a cloud of solid/melted/vaporised fragments; the cloud expands along the stand-off, distributing the impact momentum over a large area of the second sheet. However, to cope with the increase in space debris (and with the severe safety requirements as well), the standard Whipple shield configuration has to be replaced by innovative and more effective protections. At present, targets composed of three walls, using advanced materials (Kevlar™, Nextel™,

composites, etc.) are under investigation[2,3]. An "all aluminium" 3-wall configuration has been tested during a study performed as part of the Columbus program, under DASA/ESA contract. Aluminium projectiles have been fired against the target at 7 km/s. Unfortunately, the experiments have shown that this target has a low ballistic efficiency owing to a strong spallation phenomenon of the thick intermediate bumper shield. The present paper aims at assessing the capability of using the non-linear explicit finite-differences computer code AUTODYN-2D to simulate the complex ballistic behaviour of a metallic 3-wall system under hypervelocity impacts. Phase changes (solid to gas transitions) and elasto-plastic behaviour of materials subjected to large strains, large strain-rates and high temperatures were taken into account and simple failure models were also included in the calculations. Projectile, bumper shields and back-up wall were modelled by four different interacting Lagrangian grids with an erosion algorithm that retains the eroded nodes. The hydrocode simulations are compared with the experimental data.

2 Experimental results

The hypervelocity test has been performed at the Ernst Mach Institute in Freiburg (D), using the two-stage, Large Light Gas Gun (LLGG). The target was composed of a 150 mm x 150 mm, 2.5 mm thick 6061-T6 aluminium plate (the first bumper shield) separated from a second 300 mm x 300 mm, 6 mm thick 6061-T6 aluminium plate (the second bumper shield) by a stand-off of 90 mm. A third 300 mm x 300 mm, 3.2 mm thick 2219-T851 aluminium plate (the back-up wall) was placed at a stand-off of 42 mm from the second bumper shield. The plates were held by steel bars and frames. The projectile used was a 10 mm diameter aluminium (Al F37) sphere with a velocity of 7 km/s, normal impact. Although the typical average velocity of orbital debris impacting on a spacecraft in Low Earth Orbit is about 10 km/s, Light Gas Gun hypervelocity tests for projectiles in excess of 1 g are limited to velocities below 7 km/s.
In Figure 1, a triple exposed X-ray picture shows the evolution of the debris cloud between the first and second plate, and the spall fragments caused by the spallation of the second bumper shield hitting the back-up wall at a later time. The velocity of the front of the debris cloud was measured to be about 6.3 km/s. The velocity of the ejected spall fragments could not be resolved with a good precision, but it is in the range of 0.8÷0.9 km/s.
The damage description is summarised in Table 1. In the same table the results of the numerical calculations are reported for comparison (the numerical results are discussed in the following paragraph).

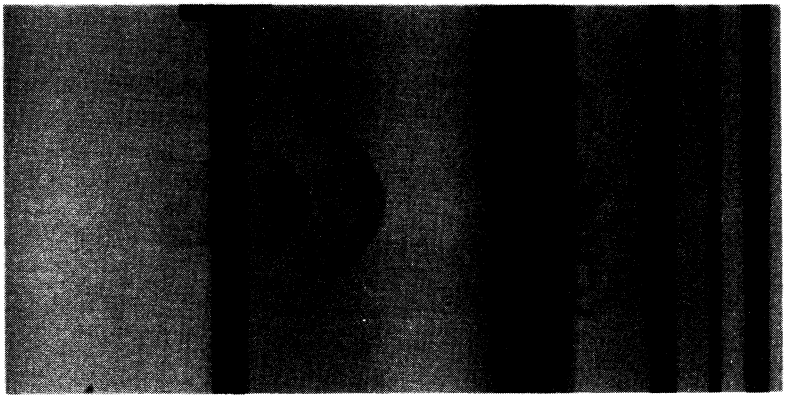

Figure 1: LLGG experiment No. 8144. X-ray pictures at 3.6, 9.3 and 70.6 μs.

Table 1: Damage description. 10 mm Al sphere at 7 km/s, normal impact.

Target Plate	Thickness (mm)	Stand -off (mm)	Diameter of damaged area (mm)	Hole diameter (mm)	Debris Cloud and spall fragments velocity (km/s)
Expt. No.8144			Autodyn Expt. run01 run02	Autodyn Expt. run01 run02	Autodyn Expt. run01 run02
1st Bumper Shield	2.5	0	None	22.0 21.5 **21.6**	6.3 6.4 **6.3**
2nd Bumper shield	6	90	230 240 **200** spall diameter 54 43 **60**	4.2 6.1 **4**	0.75 0.86 **0.8-0.9**
Back-up wall	3.2	42	damaged area 62 61 **55**	1.4 2.5 **3**	None

Note: run01-Erosion strain 2.5; run02-Erosion strain 2.0.

3 Numerical results

AUTODYN code

The AUTODYN capability of modelling space debris impacts has already been extensively demonstrated by several authors[4,5,6]. Lagrange, Euler, ALE (Arbitrary Lagrange Euler) and Shell processors are available in AUTODYN-2D. The Lagrange processor, in which the grid distorts with the material, has the advantage of being computationally fast and gives a good definition of the material interfaces. The ability of the Lagrangian (i.e., Lagrange, ALE and Shell) processors to simulate impact problems with large deformations can be enhanced by the use of an erosion algorithm that works removing Lagrangian cells which have reached a user-specified strain, typically in the range between 150% and 300%[6]. In AUTODYN the user can choose to discard or retain the mass and momentum of nodes associated with discarded cells. Since the very distorted cells are automatically removed from the calculation, the use of the erosion algorithm avoids tedious interactive re-zonings.

Material models

Strength models For the analysis reported here, both the Steinberg[7] and the Johnson-Cook[8] strength models were used. In the Steinberg model, the shear modulus and yield strength are functions of plastic strain, pressure and internal energy (temperature). Even if there is not a direct dependence on the strain rate, the predictions of that model were successfully compared with the measured stress and free-surface velocity versus time data for a number of shock wave experiments[7]. On the other hand, the Johnson-Cook model accounts also for the influence of the strain rate, but the maximum strain rates in the experimental conditions at which the Johnson-Cook data are derived, are of the order of 10^3 s^{-1}.

For Al6061 (first and second bumper shields), the available data of the Steinberg model was used as well as for AlF37 (projectile) with modification of the yield strength and the maximum yield. For Al2219 (back-up wall) the available data of the Johnson-Cook model for Al2024 was used with some modifications for the influence of strain and temperature.

Table 2 lists the material properties used in the calculations.

Table 2 Material Properties

Material property	Al 6061 T6	Al 2219 T851	Al F37
Equation of State	**Tillotson** coefficients from Ref.2	**Tillotson** coefficients from Ref.2 for Al6061-T6 with ρ = 2.840 (g/cm3)	**Tillotson** coefficients from Ref.2 for Al6061-T6 with ρ = 2.850 (g/cm3)
Strength Model	**Steinberg** coefficients from Ref.4 with Y0 2.90E5 (kPa) Ymax 6.80E5 (kPa)	**Johnson-Cook** G 2.76E7 (kPa) A 3.45E5 (kPa) B 1.10E6 (kPa) n 1.0 C 1.5E-2 m 0.8 Tmelt 775 (°K)	**Steinberg** coefficients from Ref.4 with Y0 2.50E5 (kPa) Ymax 3.70E5 (kPa)
Failure criterion	Pmin -1.2E6 (kPa) Erosion geometric strain 2(run02) 2.5(run01)	Pmin -1.2E6 (kPa) Erosion geometric strain 2(run02) 2.5(run01	Pmin -1.2E6 (kPa) Erosion geometric strain 2(run02) 2.5(run01

Equation of state The Tillotson[9] equation of state was used in order to take into account the phase changes by modelling a solid to gas transition of the materials during the hypervelocity impact phase. The correct prediction of this phase is important because it determines the shape and the status of the aluminium sphere in the debris cloud and consequently the effects of the debris cloud itself on the second bumper shield.

Failure criteria The Lagrangian processor together with the erosion algorithm were used. The values used for the erosion strain (geometric) were 250 and

200% (run01 and run02 of Table 1, respectively) for all of the three materials. Both mass and momentum of the eroded nodes were retained in order to simulate the interaction of the debris cloud fragments with the second bumper plate. The use of the geometric erosion strain criterion in the algorithm permitted also a failure criterion to be introduced in order to simulate the spallation type fracture. The bulk failure criterion, in which the failure is triggered by the appearance of the maximum tensile (or negative) hydrostatic pressure (P_{min}), was used.

Comparison with the experimental results

Figure 2 shows the two-dimensional axisymmetric geometric configuration used in the two numerical analyses (run01 and run02). The experimental square targets were approximated in our calculations by circular plates with equivalent areas. The displacements of each plate were constrained in all directions at the external boundaries in order to model the bolt-on constraint.

A very fine mesh was used for all the four Lagrangian subgrids, the cell size ranging between 0.18 mm for the first bumper shield and 0.25 mm for both the second bumper and the back-up wall. The 10 mm sphere was modelled by using 630 cells. The total number of cell used in the analysis was 7170.

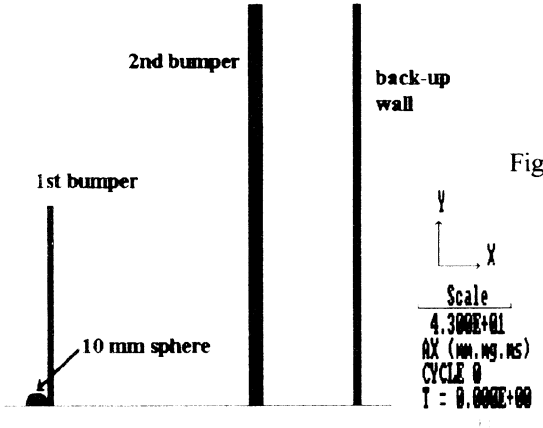

Figure 2: Geometrical modelling

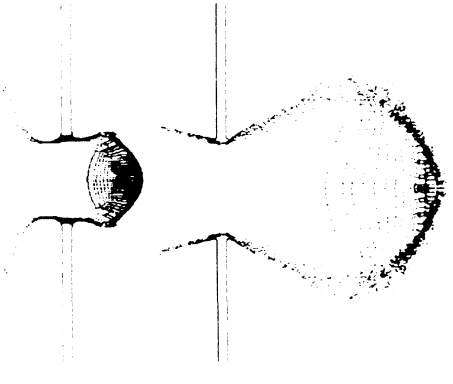

Figure 3: Run02 - Debris cloud at 3.6 and 9.3 μs after the impact of the Al sphere on the 1st bumper shield.

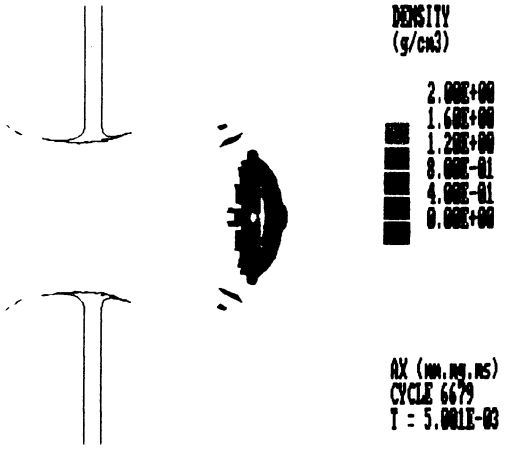

Figure 4: Run02 - Fragmentation of the projectile (after 5 μs).

Phase 1: formation and evolution of the debris cloud. Figure 3 shows the debris cloud formation at an early stage for run02 (for run01 the results are very similar): the projectile completely perforates the first bumper shield producing a hole with a diameter between 22.0 (run01) and 21.5 mm (run02) to be compared with the hole measured in the test (21.6 mm). In Figure 4, a density plot is also shown in which the incipient spall effect in the rear part of the projectile is evident. This phenomenon, also found in experiments carried out by Piekutowski[10], is in part responsible for the projectile fragmentation.
The numerical debris cloud calculations are in a fairly good agreement with the X-ray pictures reported in Figure 1. Moreover the calculations give a value of the velocity of the front part of the cloud (the fastest one) between 6.3 (run01) and 6.4 km/s (run02). X-ray measurements give a front cloud velocity of 6.3 km/s: the agreement in this case is very good.

Phase 2: interaction of the debris cloud with the second bumper shield
The last stage of the debris cloud flight and the interaction with the second bumper shield are shown in Figure 5. The impact time of the debris cloud against the second bumper calculated with AUTODYN agrees very well with the experimental one (run01: 14.8 μs, run02: 14.6 μs, experiment: 14.2 μs).
The fragments damage the second bumper shield for diameters of 230 mm (run01), 240 mm (run02) and create holes of 4.2 and 6.1 mm diameter (for run01 and run02, respectively); experimental data is 200 mm and 4 mm. The shock inside the second target produces a spalling and several low velocity fragments are generated, with calculated velocities of 0.75 km/s (run01), 0.86 km/s (run02). The experimental velocity is 0.8÷0.9 km/s.
In Figure 6 the final shapes of the 2nd bumper shield obtained in run01 and run02 (at about 200 μs) are compared with the experimental shape: the

diameter of the spall damaged zone is slightly under-predicted: theory 54 and 43 mm (run01 and run02, respectively); experiment 60 mm.

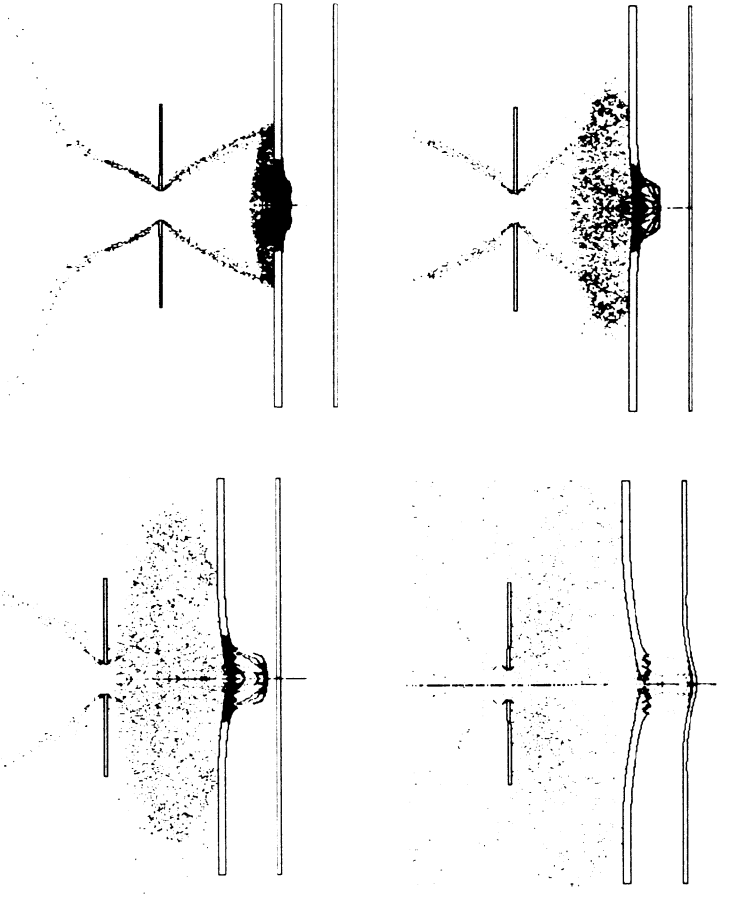

Figure 5: Run01 - Interaction of the debris cloud with the 2nd bumper shield. Production of spall fragments and interaction with the back-up wall (times: 25,40,60 and 150 μs).

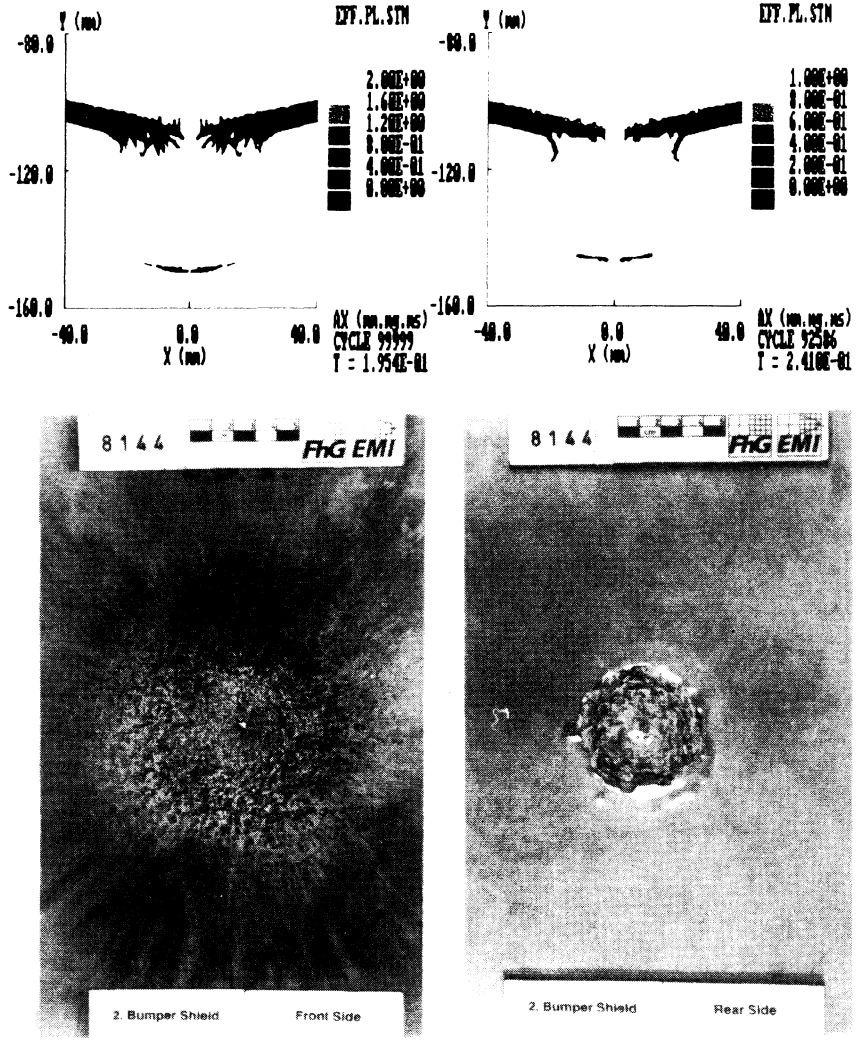

Figure 6: Comparison of the theoretical final shapes of the 2nd bumper shield (top left: Erosion strain 2.5; top right: Erosion strain 2.0) with the experimental damage (bottom left: front plate; bottom right: rear plate).

Phase 3: interaction of the spall fragments with the back-up wall In Figure 7 the damage produced by the flying spall fragments on the back-up wall is shown in terms of equivalent plastic strain contour plots for the two simulations. In the same Figure, the final experimental shape of the back-up wall is also shown for comparison: the theory predicts damaged areas with diameters of 62 and 61 mm with holes of 1.4 and 2.5 mm (run01 and run02, respectively); the experiment gives a 55 mm damaged area and a 3 mm hole.

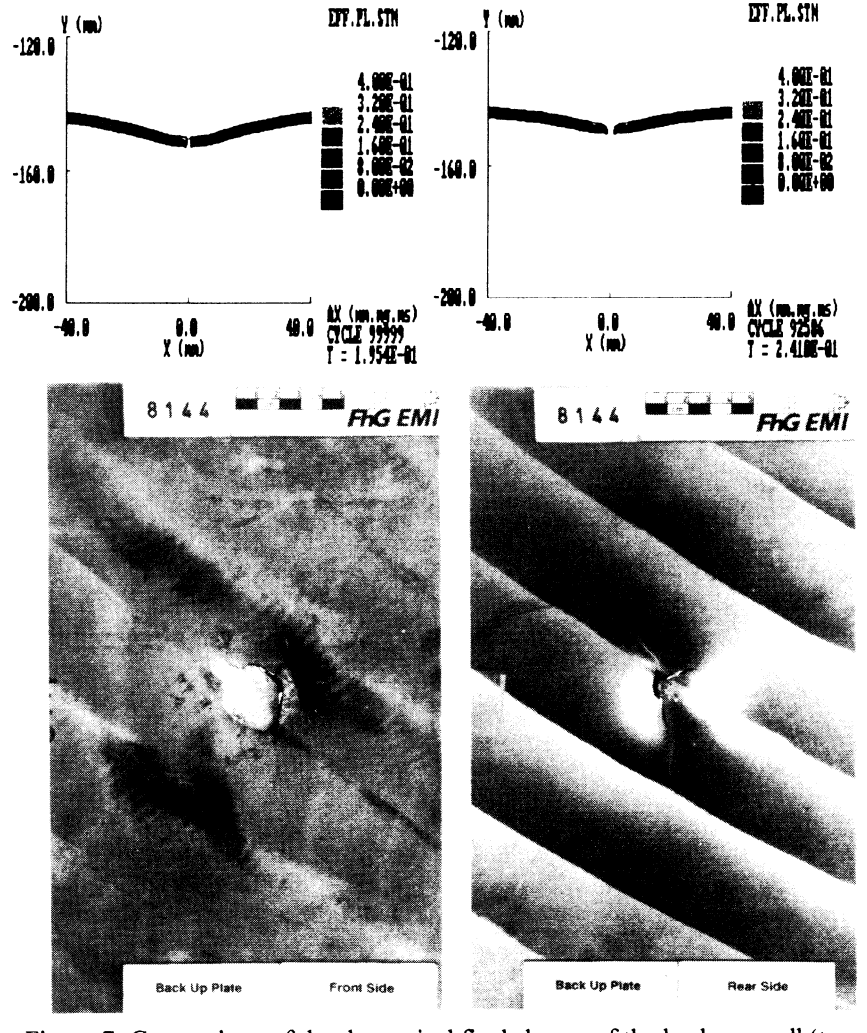

Figure 7: Comparison of the theoretical final shapes of the back-up wall (top left: Erosion strain 2.5; top right: Erosion strain 2.0) with experimental damage (bottom left: front plate; bottom right: rear plate).

4 Conclusions

The AUTODYN-2D hydrocode has been used to model the hypervelocity impact of a spherical, aluminium projectile hitting, at 7 km/s, a three-wall aluminium target under investigation for the protection of a spacecraft against orbital debris. The simulation used a Lagrangian processor combined with an erosion algorithm, standard equation of state (Tillotson) and constitutive material models (Steinberg and Johnson-Cook). A fairly good correlation with a

Light Gas Gun experiment was obtained, and the various and complex physical phenomena typical of hypervelocity impacts against a multiple, spaced target were correctly predicted. A good agreement was reported especially for the debris cloud shape and front velocity, and for the main damage mechanism of the second wall, which showed a strong spallation upon impact with the debris cloud. The velocity of the fragments spalled and detached from the rear side of the second bumper was also correctly simulated. The failure of the back-up wall is typical of a low velocity impact, with asymmetric radial cracks which cannot be properly simulated by a 2-D, axial-symmetric code. Two values of the erosion threshold (250% and 200%) were investigated. A better correlation, from both the qualitative and quantitative point of view, was reported when the higher erosion strain was used.

5 References

1. Cowler, M., et al., AUTODYN - An interactive non linear dynamic analysis program for microcomputers through supercomputers, *9th International Conference on Structural Mechanics in Reactor Technology*, Lausanne, 1987.
2. Christiansen E.L., et al., Enhanced Meteoroid and Orbital Debris Shielding, *Proceedings of the 1994 Hypervelocity Impact Symposium*, Santa Fe, 1994.
3. Destefanis, R., Faraud M., Meteoroid and debris impacts on manned modules: complexity, uncertainties and heavy shield design, *46th International Astronautical Congress*, Oslo, 1995.
4. McDonnel, J.A.M., et al., Hydrocode modelling in the study of space debris impact crater morphology, pp. 425-431, *Proceedings of First European Conf. on Space Debris*, Darmstadt, 1993.
5. Hayhurst, C.J., et al., Modelling of microparticles hypervelocity oblique impacts on thick targets, pp. 375-386, *Proceedings of the 1994 Hypervelocity Impact Symposium*, Santa Fe, 1994.
6. Katayama, M. A, et al., Numerical simulation method and its verification for space debris impacts on the Whipple shield, *46th International Astronautical Congress*, Oslo, 1995.
7. Steinberg, D.J., Equation of state and strength properties of selected materials, *UCRL-MA-106439, Lawrence Livermore Nat. Lab.*, Livermore, 1991.
8. Johnson, G.R., Cook, W.H., A constitutive model and data for metals subjected to large strains, high strain rates and high temperatures, *Proceedings of the 7th Int. Symposium on Ballistics*, The Hague, 1983.
9. Tillotson, J.M., Metallic equation of state for hypervelocity impact, *GA-3216, General Atomic*, San Diego, 1962.
10. Piekutowski, A.J., Fragmentation of a sphere initiated by hypervelocity impact with a thin sheet, pp. 627-638, *Proceedings of the 1994 Hypervelocity Impact Symposium*, Santa Fe, 1994.